JOURNAL OF AIRCRAFT
Vol. 36, No. 6, November–December 1999

Aileron Effectiveness at High Angles of Attack: Interaction with Forebody Blowing

Nelson Pedreiro,* Yuji Takahara,† and Stephen M. Rock‡
Stanford University, Stanford, California 94305

An experimental investigation has been conducted to determine the effectiveness of ailerons in the high angle-of-attack regime in the presence of forebody tangential blowing. Forebody blowing generates both roll and yaw moments, but independent control of these moments requires the use of a second actuator. Results from this study support the idea of using ailerons and forebody blowing for aircraft roll and yaw control at high angles of attack. Experiments were conducted at 45-deg nominal incidence angle, using a wind-tunnel model configuration consisting of a cone–cylinder fuselage and a delta wing. The effectiveness of the ailerons as a function of aileron area has been determined. It is shown that increasing aileron size beyond a certain limit produces only marginal increase in the capability of generating roll moment. Cross-coupling effects on pitch and yaw moments due to aileron deflection and the combined effects of aileron deflection and blowing are presented. Results show that the effects of starboard and port-side control surfaces are nearly uncoupled.

Nomenclature

b = wing span
b_A = span or length of a single aileron
C_l = roll moment coefficient, $M_x/q_\infty S_{\text{ref}} b$
C_m = pitch moment coefficient, $M_y/q_\infty S_{\text{ref}} \bar{c}$
C_n = yaw moment coefficient, $M_z/q_\infty S_{\text{ref}} b$
C_μ = jet momentum coefficient, $\dot{m}_j V_j/q_\infty S_{\text{ref}}$
c_A = chord of aileron
$\bar{c}$ = mean aerodynamic chord
M_x = roll moment
M_y = pitch moment
M_z = yaw moment
$\dot{m}_j$ = jet mass flow rate
P = intersection of ϕ axis and γ axis
q_∞ = dynamic pressure, $\rho_\infty U_\infty^2/2$
S_A = planform area of ailerons, $2b_A c_A$
S_{ref} = reference area, wing planform area
U_∞ = freestream air speed
V_j = air jet speed at exit of blowing slot
γ = second degree of freedom
ρ_∞ = freestream air density
ϕ = first degree of freedom, roll

Introduction

EXPANSION of the flight envelope into the poststall regime can provide a tactical advantage to fighter aircraft and an improved performance during takeoff and landing for future high-speed transport aircraft. The main difficulty associated with operation in these flight regimes is the loss of aerodynamic control power, mainly, yaw control. As the angle of attack increases, the vertical tail is immersed in separated flow and loses its capability of generating yaw moment. This occurs when yaw control is most needed to counter large yaw moments due to asymmetric flow development. Therefore, augmented control is required for aircraft operation at high angles of attack. Recent studies[1,2] have identified active flow control as a critical area that could provide the required control augmentation. It is expected that the use of active flow control techniques can lead to configurations with reduced takeoff gross weight, improved low-observables characteristics, and high maneuverability at high angles of attack.

Various methods of active flow control have been proposed.[3–10] In particular, Adams et al.[11] have shown, through simulation, that forebody blowing can be used for flight envelope expansion. Pedreiro et al.[12] have successfully demonstrated the use of forebody tangential blowing (FTB) to control a tailless wind-tunnel model in roll and yaw using blowing as the only actuator, and Takahara and Rock[13] have developed an approach for robust control design using FTB. Forebody blowing is a very efficient actuator that relies on flow amplification effects to generate both roll and yaw moments; however, independent control of roll and yaw requires the use of a second actuator. Conventional control surfaces are likely candidates, but the interaction of forebody blowing with these surfaces needs to be understood before augmented control laws for real aircraft can be designed.

Most of the work to date assumes that the effect of active flow control is incremental, that is, moments generated by active flow control techniques are added to the moments generated by conventional control surfaces. It is not clear that this assumption should be valid. In fact, it has been shown[14] that FTB changes the aerodynamic characteristics (stability derivatives) of the vehicle. Therefore, control augmentation using FTB requires an understanding of its effects on the vehicle aerodynamics. Furthermore, the interactions of blowing with conventional control surfaces are not easily determined.

The purpose of this work is to investigate some of these interactions. In particular, an experimental investigation was conducted to determine the interaction between FTB and the ailerons. The effectiveness of ailerons in the high angle-of-attack regime and their interactions with FTB have been determined experimentally. A wind-tunnel model consisting of a cone–cylinder fuselage and a sharp leading-edge delta wing with 60-deg sweep angle was used in the experiments (Fig. 1). Measurements of the static aerodynamic loads were performed at 45-deg nominal angle of attack and 25 m/s freestream speed. The effects of forebody blowing and aileron deflections have been determined, as well as the effects of varying the area of the ailerons.

Specifically, five sets of experimental data were collected: 1) roll and yaw moments due to aileron deflection; 2) roll and yaw moments due to blowing; 3) roll moment for various aileron sizes; 4) roll, yaw, and pitch moments due to independent deflection of starboard and

Presented as Paper 98-4518 at the AIAA Atmospheric Flight Mechanics Conference, Boston, MA, 10–12 August 1998; received 18 January 1999; revision received 18 May 1999; accepted for publication 19 May 1999.

*Postdoctoral Fellow, Department of Aeronautics and Astronautics; nelson@sun-valley.stanford.edu.
†Ph.D. Candidate, Department of Aeronautics and Astronautics; takahara@sun-valley.stanford.edu.
‡Associate Professor, Department of Aeronautics and Astronautics; rock@sun-valley.stanford.edu.

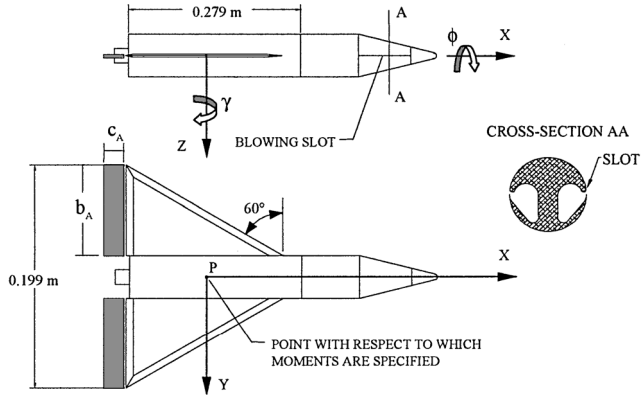

Fig. 1 Wind-tunnel model: detail of blowing slots and control surfaces.

port-side control surfaces; and 5) roll, yaw, and pitch moments due to combined effect of aileron deflection and FTB.

Experiments 1 and 2 addressed the soundness of the idea of using ailerons and FTB to control, respectively, roll and yaw at high α. The data not only show the known facts that ailerons generate considerable roll moment and FTB considerable yaw moment, but also that the adverse yaw due to ailerons is small when compared with the yaw moment capability of FTB. Similarly, roll due to FTB can be counteracted by the ailerons.

Experiment 3 addressed the design issue of aileron sizing in the high α regime. In particular, the effectiveness of the ailerons as a function of aileron area has been determined.

Experiment 4 explored different strategies of using the control surfaces. The experiment shows that deflecting just one control surface trailing edge up generates 75% of total roll moment, almost no adverse yaw moment, but considerable change in pitch moment. Moreover, the results show that the effects of the control surfaces are nearly uncoupled and can be superimposed. This is very important as it can reduce significantly the amount of data required to characterize the system.

Experiment 5 explored the interaction of FTB and ailerons. This experiment addressed the same question addressed by experiments 1 and 2, but goes a step further by showing the combined effects of FTB and ailerons. It also provides some insight on the complexity that may result in the control logic because the effects on yaw moment cannot be superimposed.

In the following sections the experimental apparatus is described and the experimental results are presented in detail. The overall conclusion they support is that ailerons and forebody blowing can be used to control an aircraft in roll and yaw in the high angle-of-attack regime.

Experimental Apparatus

Wind Tunnel and Model

The wind-tunnel facility of the Aeronautics and Astronautics Department at Stanford University was used for these experiments. It consists of a closed-circuit low-speed wind tunnel with 0.45×0.45 m test section. The maximum freestream air speed in the test section is 50 m/s.

The wind-tunnel model used in the experiments is shown in Fig. 1. It consists of a sharp leading-edge delta wing with 60-deg sweep angle and a cone–cylinder fuselage. In these experiments a round forebody tip, with radius equal to 0.00254 m, was used to decrease flow asymmetry at symmetric flight conditions and to improve repeatability of the aerodynamic loads.[15] Slots through which blowing is applied are present on both sides of the conical forebody. Air is provided to the forebody plena through flexible tubing that enters the model through the rear end of the fuselage. Control surfaces, flaps and ailerons, can be attached to the wing trailing edges and cover their full length, as shown in Fig. 1. In this study, control surfaces with a fixed span, $b_A = 0.079$ m, but various chord lengths c_A, were used to determine the effectiveness of the ailerons as a function of aileron size.

Table 1 Characteristics of the various control surfaces

Aileron chord c_A, mm	Reference area S_{ref}, m^2	Aileron area S_A/S_{ref}, %
14	0.0191	12
17	0.0197	14
20	0.0203	16
24	0.0211	18
27	0.0217	20

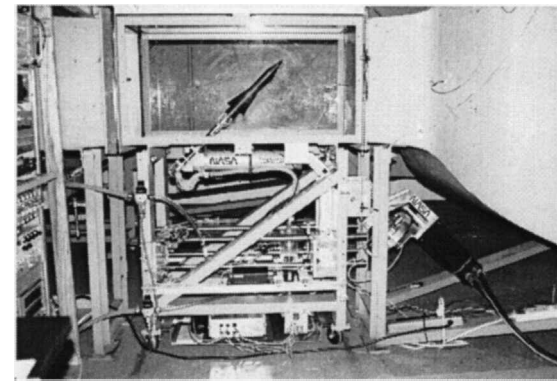

Fig. 2 Side view of test section and two-degrees-of-freedom model support system.

Table 1 contains the values of the chords of the various ailerons used, as well as their planform areas S_A, expressed as a percentage of the reference area S_{ref}, which is defined as the planform area of the wing including the control surfaces. The range of aileron sizes used in the experiments was chosen around the value of S_A/S_{ref} of 15%. This value is typical of the trailing-edge control surfaces on such aircraft as the Mirage 2000. Also included in Table 1 are the values of S_{ref} that are used to compute the nondimensional aerodynamic loads. The percentage areas shown in Table 1 are used throughout the paper to designate the various ailerons.

Tests were conducted at 25 m/s and a nominal incidence angle of 45 deg. The Reynolds number based on the wing root chord (no control surfaces) is 3.333×10^5. Tunnel blockage at the nominal configuration with no control surfaces attached is 9%. Figure 2 shows the model attached to the supporting mechanism.

Model Support System

A unique support system that constrains the model to two degrees of freedom, roll and yaw, was used in the experiments.[14] The apparatus can be divided into two subsystems: The first one implements the roll degree of freedom ϕ and consists of a shaft mounted on bearings. The wind-tunnel model is attached to the roll shaft allowing the model to rotate about its longitudinal axis. The roll subsystem is mounted on a mechanical arm that can rotate about an axis perpendicular to the longitudinal axis of the model (Fig. 2). The mechanical arm implements the second degree of freedom γ. Although the apparatus can be used for dynamic experiments, in this work only static experiments were conducted with the wind-tunnel model placed at various roll and yaw angles. Angles ϕ and γ relate to the angle of attack α and side slip angle β through the following equations:

$$\cos\alpha\cos\beta = \cos\alpha_0\cos\gamma$$

$$\sin\beta = \sin\alpha_0\sin\phi - \cos\alpha_0\sin\gamma\cos\phi$$

$$\sin\alpha\cos\beta = \sin\alpha_0\cos\phi + \cos\alpha_0\sin\gamma\sin\phi \qquad (1)$$

where $\alpha_0 = 45$ deg is the nominal incidence angle, that is, the angle of attack for $\phi = \gamma = 0$. Mechanical constraints limit the degrees of freedom to the following ranges: $|\phi| < 105$ deg and $|\gamma| < 30$ deg.

Air Injection System

Air can be injected independently through slots located on both sides of the conical portion of the forebody (Fig. 1). The amount of injected air is quantified by the jet momentum coefficient that is defined as

$$C_\mu \equiv \frac{\dot{m}_j V_j}{q_\infty S_{\text{ref}}} \tag{2}$$

Specially designed flowmeters[16] are used to measure the mass flow rate from which C_μ is calculated. Servovalves are used to vary the amount of injected air. The signal from the flowmeters is read into a computer that implements a closed-loop logic for C_μ control by commanding the servovalves.

Instrumentation and Data Acquisition

The two degrees of freedom, ϕ and γ, are measured by precision potentiometers. A six-component force-torque sensor connects the model to the roll shaft and is used to provide measurements of the aerodynamic loads. Flowmeters measure the amount of blowing through each plenum. Two microcomputers equipped with data acquisition boards were used in the experiments. One computer was used in the closed-loop control of C_μ, that is, to control the amount of air injected in each plenum. The second computer was used for data acquisition.

Experimental Results

Sign Conventions and Accuracy of Measurements

The following sign conventions are used: For all results presented, angles ϕ and γ are positive for rotations about the X and Z axes, as shown in Fig. 1. Roll, pitch, and yaw moments are defined as moments about the X axis, Y axis, and Z axis, respectively (Fig. 1). They are presented in nondimensional form as roll, pitch, and yaw moment coefficients, C_l, C_m, and C_n, respectively.

In this work only asymmetric blowing was used, that is, blowing was applied either on the starboard or the port side of the model but not simultaneously on both sides. Positive values of the jet momentum coefficient C_μ are used to indicate that blowing is applied to the starboard of the model, whereas negative values of C_μ are used for port-side blowing.

In regard to the deflection of the control surfaces, the main goals were to investigate their capability of generating roll moment at high angles of attack and how this capability is affected by blowing. Most of the results presented refer to the case where the control surfaces are deflected by equal amounts in opposite directions. In this case, trailing-edge-up deflection of the starboard control surface is accompanied by an equal trailing-edge-down deflection of the port-side control surface and is defined as a positive aileron deflection. Results are also presented for cases in which only one of the control surfaces was deflected. In these cases, it is explicitly stated which control surface was deflected and in which direction.

Measurements of angles ϕ and γ are accurate to within a $\frac{1}{10}$ of a degree. Errors in the values presented for the jet momentum coefficient C_μ are ± 0.0003 ($\pm\sigma$). The deflections of the control surfaces are accurate to within ± 0.25 deg. The accuracy of the measurements of roll, pitch, and yaw moment coefficients (C_l, C_m, and C_n) are, respectively, ± 0.0008, ± 0.0085, and ± 0.0054. The effects of the air supply tubing on the measurements of the aerodynamic loads are negligible.[14]

Discussion of Results

The effects of aileron deflection on the roll and yaw moment coefficients are shown in Fig. 3. Curves are shown for C_l and C_n vs roll angle ϕ, for $\gamma = 0$ and for various deflections of the ailerons. In this case, the area of the ailerons was 12% of the wing planform area

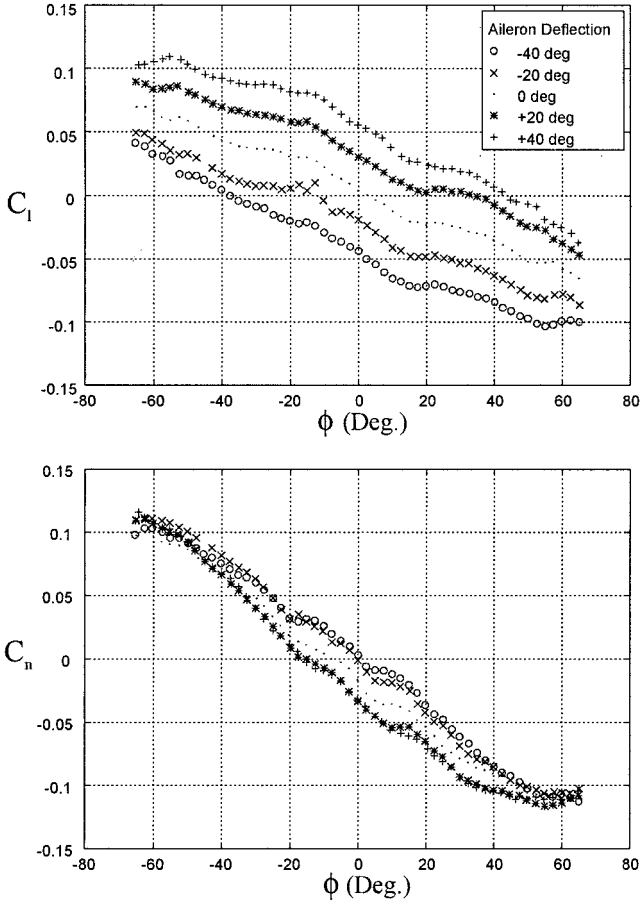

Fig. 3 Roll and yaw moment coefficients, C_l and C_n, vs ϕ, for $\gamma = 0$ and various deflections of the ailerons; aileron area is 12% of S_{ref}.

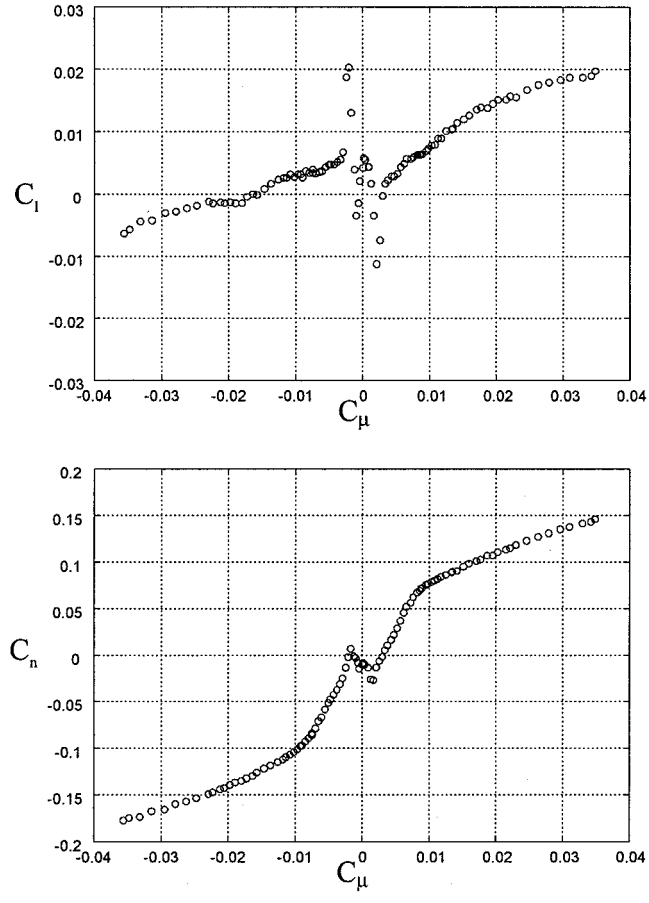

Fig. 4 Roll and yaw moment coefficients, C_l and C_n, vs C_μ for $\phi = \gamma = 0$ and no deflection of the ailerons; aileron area is 14% of S_{ref}.

S_{ref}. It is seen that a 20-deg aileron deflection produces a change in roll moment that is slightly larger than the roll moment variation due to a 20-deg change in roll angle. It is reasonable to assume that this significant change in roll moment caused by aileron deflection is mainly due to the contribution of the pressure side of the wing and control surfaces because the flow is separated on the leeside of the vehicle. The effect of deflecting the ailerons is approximately a shift in the roll moment curve. Furthermore, for a broad range of roll angles, a deflection of the ailerons of 40 deg causes a variation in roll moment that is almost two times the variation obtained with 20-deg deflection of the ailerons.

Changes in yaw moment caused by the deflection of the ailerons are larger for roll angles between −20 and 20 deg and decrease as the absolute value of the roll angle increases. These changes are smaller than the changes observed in roll moment for the entire range of roll angles. Increasing the deflection of the ailerons from 20 to 40 deg does not cause significant change in the yaw moment, which is in sharp contrast with the roll moment behavior. The nonzero values of the roll and yaw moment coefficients for zero roll and yaw angles shown in Fig. 3 for the case of no aileron deflection are significant, especially the value of −0.02 for the yaw moment coefficient. This is typical at high angles of attack and is caused by the asymmetric flow that develops over the conical forebody. It should be noted that the asymmetry would be much more severe if a forebody with a sharp tip had been used.[15]

Figure 4 contains curves for the roll and yaw moment coefficients vs C_μ for $\phi = \gamma = 0$ and no deflection of the ailerons. Comparison of these curves with the results shown in Fig. 3 shows that the yaw moments generated by the deflection of the ailerons (adverse yaw) are a small fraction of the yaw moments that can be generated by blowing. Furthermore, the maximum value of the roll moment generated by blowing can be achieved with a deflection of the ailerons that is less than 20 deg. These results support the idea of using ailerons and forebody blowing to control roll and yaw at high angles of attack.

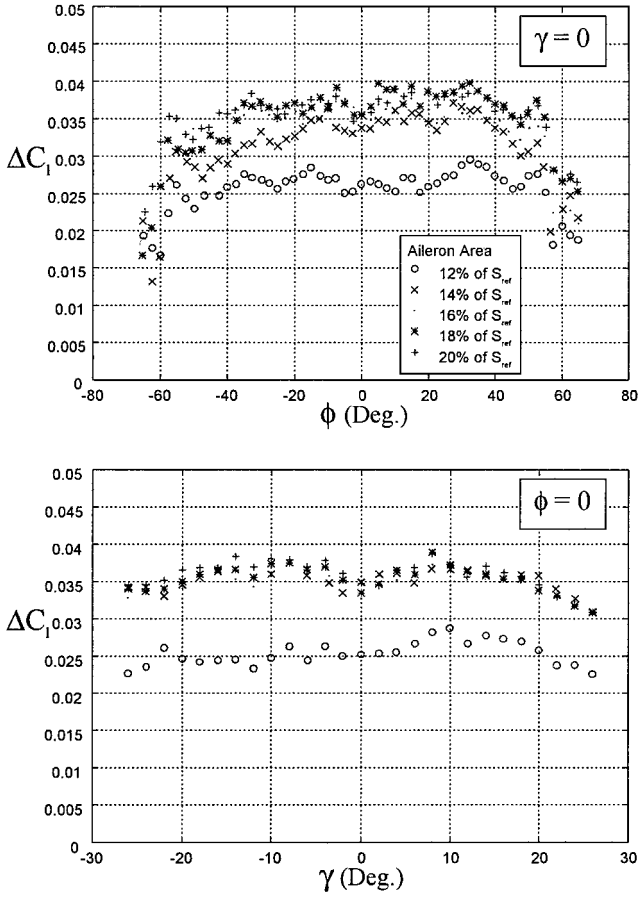

Fig. 5 Change in roll moment coefficient ΔC_l vs ϕ and γ, for a 20-deg aileron deflection and ailerons of various sizes.

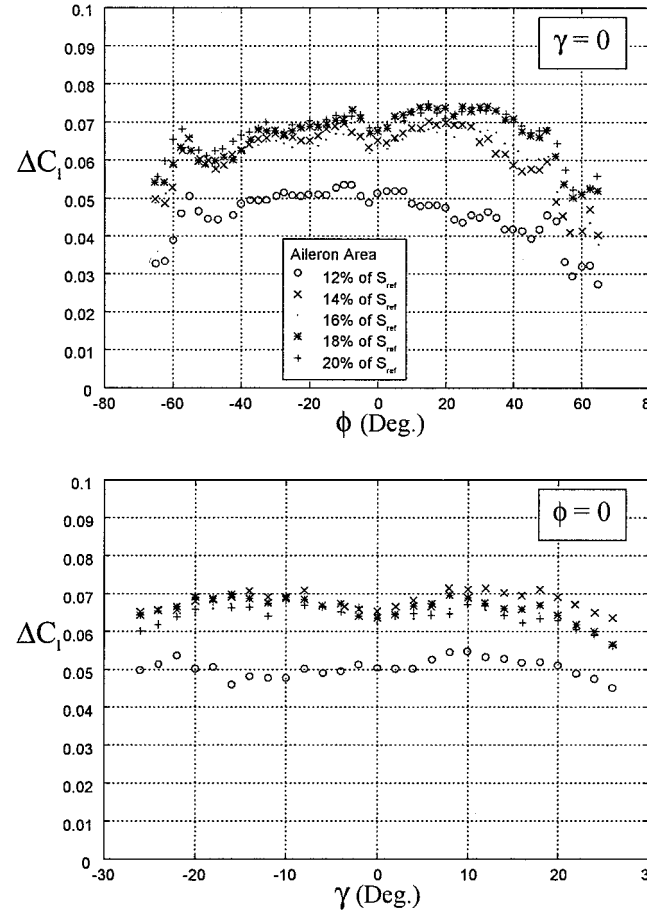

Fig. 6 Change in roll moment coefficient ΔC_l vs ϕ and γ, for a 40-deg aileron deflection and ailerons of various sizes.

The variation in the roll moment coefficient ΔC_l due to a 20-deg deflection of the ailerons is presented in Fig. 5 vs roll and yaw angles for ailerons of various sizes. It is seen that a significant increase in ΔC_l occurs when the area of the ailerons increases from 12% of S_{ref} to 14% of S_{ref}. On the other hand, increasing the area of the ailerons to more than 14% of S_{ref} does not produce significant increase in ΔC_l. As shown in Fig. 6, similar results are obtained for a 40-deg aileron deflection. These results are consistent with the assumption that at high angles of attack the roll moment due to aileron deflection is mainly generated by flow changes in the pressure side of the vehicle. Qualitatively similar results can be obtained with a simulation of a two-dimensional thin airfoil with flaps of various chords where only the changes in pressure distribution on the pressure side are considered. The largest changes in pressure distribution due to flap deflection occur near the hinge point, and therefore, portions of the flap farther away from the hinge point are less effective.

In summary, increasing aileron size increases the roll moment that can be generated, but the effectiveness of the aileron, measured as the ratio of the roll moment that can be generated over the size of the aileron required to generate it, will decrease for large ailerons. For the configuration used in these experiments and a nominal angle of attack of 45 deg, the most effective aileron size is approximately 14% of S_{ref}.

The effects of deflecting the starboard and port-side control surfaces independently are shown in Fig. 7. In this case, roll, pitch, and yaw moment coefficients are plotted vs roll angle, for $\gamma = 0$. The data refer to an aileron with area equal to 16% of S_{ref}. Data are shown for the following cases: 1) no deflection of the control surfaces (circles); 2) positive 40-deg aileron deflection, that is, starboard control surface deflected 40 deg trailing edge up and port-side control surface deflected 40 deg trailing edge down (×); 3) only the starboard control surface deflected 40 deg trailing-edge up (asterisk); and 4) only

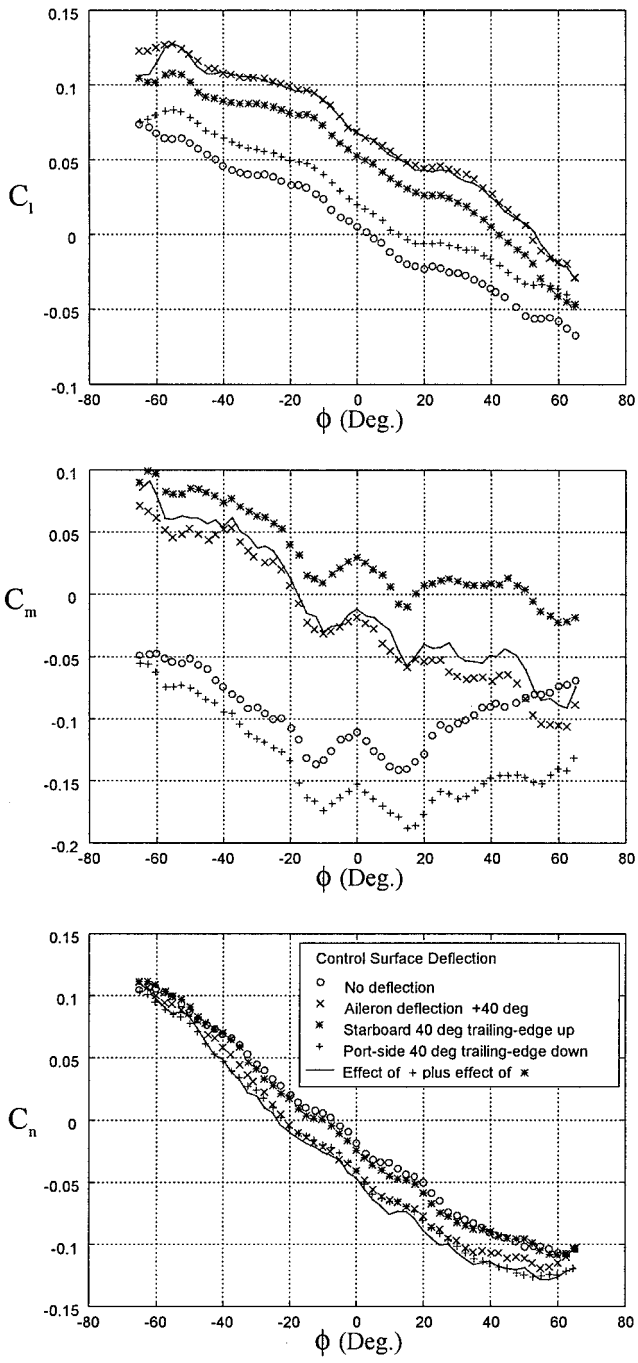

Fig. 7 Effect of deflecting starboard- and port-side control surfaces independently. Roll, pitch, and yaw moment coefficients, C_l, C_m, and C_n, vs ϕ, for $\gamma = 0$; aileron area is 16% of S_{ref}.

the port-side control surface deflected 40 deg trailing edge down (plus). Also shown in Fig. 7 are curves (solid) obtained by adding the effects of deflecting a single control surface at a time, that is, the variation in moment coefficients caused by case 3 plus the variation caused by case 4.

It is seen that, for most of the roll angle range, approximately 75% of the roll moment is generated by the control surface that is deflected toward the leeside of the vehicle (trailing edge up). This is attributed to the nonlinear characteristics of the flow on the pressure side caused by the large angle of attack and large deflections of the control surfaces. Although this suggests that, in terms of generating roll moment, it is preferable to deflect only one of the control surfaces, it is also necessary to examine the behavior of the pitch and yaw moments. Because the goal is to use the ailerons to generate roll moment, pitch and yaw moments represent cross-coupling effects that should be minimized. The results show that lower values are obtained for the change in pitch moment for the case where the two control surfaces are deflected (case 2) as compared to the case of trailing-edge-up deflection of the starboard control surface (case 3). This favors the simultaneous deflection of both control surfaces. On the other hand, minimum adverse yaw moment occurs for the case of trailing-edge-up deflection of a single control surface (case 3). Therefore, deflection of a single control surface toward the leeside (trailing edge up) is more effective in generating roll moment and produces less adverse yaw moment and larger variations in pitch moment, whereas simultaneous deflection of both control surfaces generates larger variations in yaw moment and smaller variations pitch moment.

Comparison of the curves obtained by adding the effects of deflecting a single control surface at a time with the data for the case

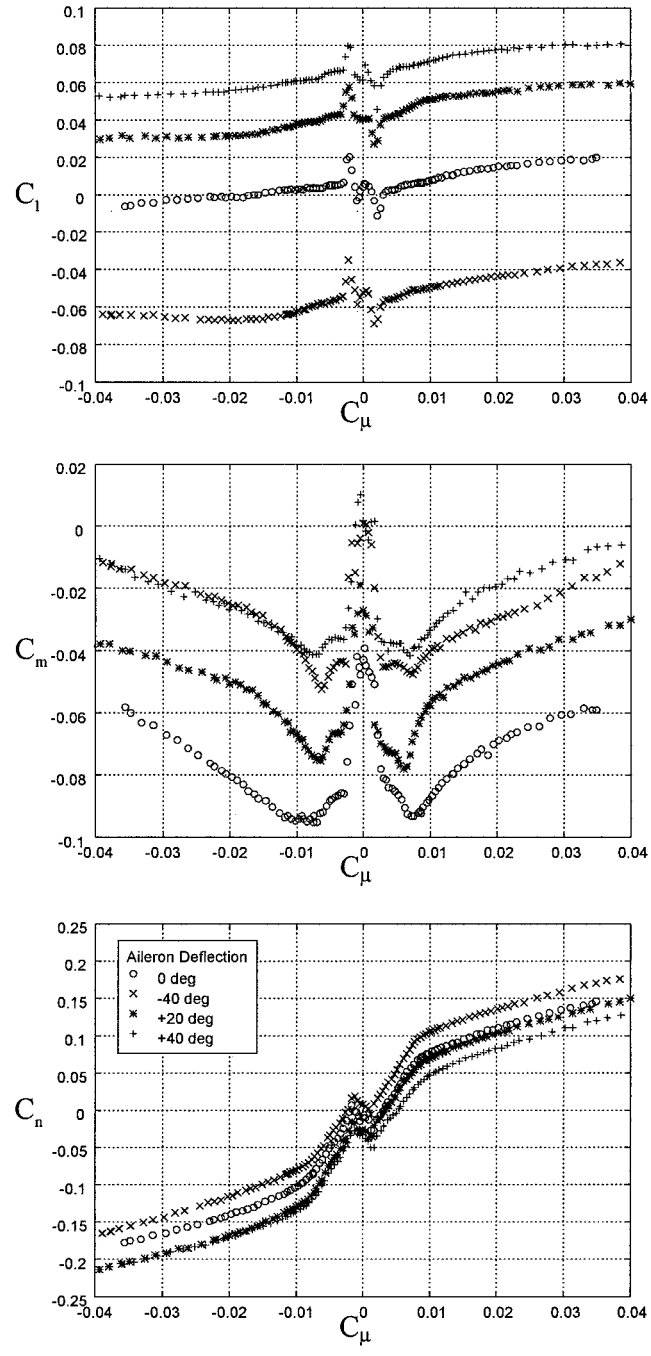

Fig. 8 Combined effect of forebody blowing and aileron deflection. Roll, pitch, and yaw moment coefficients, C_l, C_m, and C_n, vs C_μ, for $\phi = \gamma = 0$; aileron area is 14% of S_{ref}.

where the two control surfaces were deflected simultaneously shows that the effects of the starboard and the port-side control surfaces are nearly uncoupled. To first order, their effects in the roll, pitch, and yaw moments can be added, which greatly simplifies the characterization of the control surfaces required for modeling their effects on the aerodynamic loads acting on the vehicle. The lack of a vertical tail in the wind-tunnel model can contribute to the uncoupling of the effects of starboard and port-side control surfaces.

Comparison of Figs. 3 and 7 allows some insight into the effect of aileron size in the adverse yaw moment. Increasing the aileron area from 12% of S_{ref} to 16% of S_{ref} causes a modest increase in the adverse yaw moment. Moreover, in both cases the adverse yaw is a small fraction of the yaw moment that can be generated by blowing and can be easily compensated.

The effects of FTB on the roll, pitch, and yaw moments are shown in Fig. 8, for $\phi = \gamma = 0$ and various deflections of the ailerons. Ailerons with an area equal to 14% of S_{ref} were used in these measurements. For $|C_\mu| > 0.03$, the effect of deflecting the ailerons is mainly to shift the curves of C_l vs C_μ. This means that, except for the small blowing intensities, it is a reasonable approximation to superimpose the effects of blowing and aileron deflection in the roll moment. For the pitch moment, the differences in the curves for 40- and −40-deg aileron deflection are attributed to the limited accuracy in the measurement of C_m (± 0.0085). Although the data indicate that superposition of the effects of blowing and aileron deflection in the pitch moment could be a reasonable approximation for large values of C_μ, the results are not conclusive due to the limited accuracy of the pitch moment measurements. For the yaw moment, the results show that superposition of the effects of blowing and aileron deflection is not a reasonable assumption. This is evident because the curve corresponding to 20-deg aileron deflection coincides with the curve for 40-deg aileron deflection for negative values of C_μ and is almost coincident with the curve for zero aileron deflection for positive values of C_μ.

Conclusions

Experiments were conducted to determine the effectiveness of ailerons in the high angle-of-attack regime and their interaction with FTB. For the given configuration, significant roll moment can be generated at high angles of attack through the use of ailerons. The results show that the ailerons can generate larger roll moment than the roll moment generated by forebody blowing over a broad range of roll angles. Moreover, the adverse yaw moment generated by aileron deflection is a small fraction of the yaw moment that can be generated by blowing. Therefore, adverse roll due to blowing can be compensated by the ailerons whereas blowing can easily compensate for the adverse yaw due to aileron deflection. This supports the idea of using ailerons and forebody blowing to control the motion of the vehicle in roll and yaw.

Results indicate that there is a size of the ailerons beyond which the capability of generating roll moment increases only marginally. It is shown that most of the roll moment, about 75%, is generated by the aileron that is deflected toward the leeside of the vehicle (trailing edge up). These results are consistent with the assumption that the effect of the ailerons at high angles of attack is mainly due to changes in the flow on the pressure side of the vehicle.

The effects of the starboard- and port-side control surfaces are nearly uncoupled, that is, adding the effects of deflecting each control surface separately approximates the effects of deflecting both control surfaces simultaneously. Cross coupling (pitch and yaw moments) varies significantly for the case where both control surfaces are deflected simultaneously and the cases where only the starboard or the port-side control surface is deflected. Therefore, cross coupling can be minimized by selection of a proper strategy on how to deflect the control surfaces.

Results showed that superposition of the effects of blowing and the effects of aileron deflection is valid for roll moment over a significant range of blowing intensities, but is not valid for yaw moment. Therefore, the assumption that blowing can be modeled as an incremental effect is not generally correct and indicates that proper characterization of the effects of active flow control devices is required before augmented control laws for real aircraft can be designed.

Acknowledgments

This work was supported by the NASA–Stanford Joint Institute for Aeronautics and Acoustics, NASA Grant NCC 2-55, and by the Air Force Office of Scientific Research, Grant F49620-96-1-0248.

References

[1]Alcorn, C. W., Croom, M. A., Francis, M. S., and Ross, H., "The X-31 Aircraft: Advances in Aircraft Agility and Performance," *Progress in Aerospace Sciences*, Vol. 32, No. 4, 1996, pp. 377–413.

[2]O'Neil, P. J., Nyberg, G., deTurk, R., Seal, D. W., and Grethlein, C. E., "Impact of Agility Requirements on Configuration Synthesis," NASA CR-4627, Sept. 1994.

[3]Skow, A. M., Moore, W. A., and Lorincz, D. J., *Forebody Vortex Blowing—A Novel Control Concept to Enhance Departure/Spin Recovery Characteristics of Fighter and Trainer Aircraft*, CP-262, AGARD, No. 24, 1979, pp. 24-1–24-17.

[4]Ericsson, L. E., and Reding, J. P., "Alleviation of Vortex Induced Asymmetric Loads," *Journal of Spacecraft and Rockets*, Vol. 17, No. 6, 1980, pp. 546–553.

[5]Rao, D. M., Moskovitz, C., and Murri, D. G., "Forebody Vortex Management for Yaw Control at High Angles of Attack," *Journal of Aircraft*, Vol. 24, No. 4, 1987, pp. 248–254.

[6]Ng, T. T., and Malcolm, G. N., "Aerodynamic Control Using Forebody Strakes," AIAA Paper 91-0618, Jan. 1991.

[7]Celik, Z. Z., and Roberts, L., "Vortical Flow Control on a Wing-Body Combination Using Tangential Blowing," AIAA Paper 92-4430, Aug. 1992.

[8]Celik, Z. Z., Roberts, L., and Pedreiro, N., "The Control of Wing Rock by Forebody Blowing," AIAA Paper 93-3685, Aug. 1993.

[9]Wong, G. S., Rock, S. M., Wood, N. J., and Roberts, L., "Active Control of Wing Rock Using Tangential Leading-Edge Blowing," *Journal of Aircraft*, Vol. 31, No. 3, 1994, pp. 659–665.

[10]Celik, Z. Z., Roberts, L., and Pedreiro, N., "Dynamic Roll and Yaw Control by Tangential Forebody Blowing," AIAA Paper 94-1853, June 1994.

[11]Adams, R. J., Buffington, J. M., and Banda, S. S., "Active Vortex Flow Control for VISTA F-16 Envelope Expansion," AIAA Paper 94-3681, Aug. 1994.

[12]Pedreiro, N., Rock, S. M., Celik, Z. Z., and Roberts, L., "Roll-Yaw Control at High Angle of Attack by Forebody Tangential Blowing," *Journal of Aircraft*, Vol. 35, No. 1, 1998, pp. 69–77.

[13]Takahara, Y., and Rock, S. M., "Nonlinear Control Using Forebody Tangential Blowing," AIAA Paper 98-4204, Aug. 1998.

[14]Pedreiro, N., "Experiments in Aircraft Roll–Yaw Control Using Forebody Tangential Blowing," Ph.D. Dissertation, Aeronautics and Astronautics Dept., Stanford Univ., Stanford, CA, 1997.

[15]Chow, J. K., Pedreiro, N., and Rock, S. M., "The Impact of Forebody Geometries at High-Angle-of-Attack with Forebody Tangential Blowing," AIAA Paper 98-4522, Aug. 1998.

[16]Pedreiro, N., "Development of an Apparatus for Wind Tunnel Dynamic Experiments at High-α," NASA–Stanford Joint Inst. for Aeronautics and Acoustics, TR-119, Stanford Univ., Stanford, CA, Feb. 1997.